

Upwelling mechanisms in the northwestern Alboran Sea

Tarek Sarhan ^{*}, Jesús García Lafuente ¹, Manuel Vargas ², Juan M. Vargas ,
Francisco Plaza

Departamento de Física Aplicada II, E.T.S.I. de Telecomunicación, Universidad de Málaga, Campus de Teatinos, 29071 Spain

Received 29 January 1999; accepted 17 June 1999

Abstract

From April 1996 to July 1997, a series of hydrographic surveys were carried out in the Northwestern part of the Alboran Sea to investigate the upwelling that is an almost permanent feature in this area. Simultaneously a mooring line was deployed in the north part of the eastern section of the Strait of Gibraltar to monitor the variability of the Atlantic Jet (AJ). Two mechanisms are shown to be relevant for the upwelling dynamic in the region: the southward drifting of the AJ and wind stress. A linear relation between the angle under which the Jet enters the Alboran Sea and the distance from the coastline to the front associated with the Jet has been found. This angle that has been estimated from the low passed time series of current velocity measured by the uppermost instrument of the moored line has been then used to identify the onshore–offshore excursions of the Jet. Both upwelling mechanisms are identified from hydrographic data, because each of them has associated a different type of water mass, and they take place in different locations. Wind-driven upwelling dominates in coastal zones, on the shelf, while upwelling associated with southward drifting of the AJ prevails further offshore. The amount of sub-surface water brought up to the surface by each one is of the same order. However, wind-driven upwelling contributes to the fertilization of this region in a major extent because water upwelled by wind is richer in nutrient concentration. © 2000 Elsevier Science B.V. All rights reserved.

Keywords: fronts; upwelling; surface waters; Strait of Gibraltar; Alboran Sea

1. Introduction

The Northwestern area of the Alboran Sea, off Estepona see Fig. 1, is characterised by cold surface water. It has been considered an upwelling region by many authors (Lanoix, 1974; Cano, 1977; Copin-Montegut et al., 1982; Perkins et al., 1990 among

others). The upwelling, more evident in summer when thermal contrast is stronger, is easily observed in infrared satellite images (e.g., La Violette, 1984). The region is a zone of high biologic productivity (Rodríguez et al., 1994; Rubín et al., 1995, 1997), which gives support to the existence of upwelling.

Their oceanographic characteristics are influenced by the Atlantic Jet (AJ) that enters the Alboran Sea through the Strait of Gibraltar. It flows with an estimated speed of about 1 m s^{-1} (García Lafuente et al., 1999a), and goes around the large anticyclonic gyre that usually occupies the western Alboran basin. The northern edge of the AJ is the southern bound-

^{*} Corresponding author. Tel.: +34-952-132-889; Fax: +34-952-132-849.

E-mail address: tsarhan@ctima.uma.es (T. Sarhan)

¹ E-mail: glafuente@ctima.uma.es

² E-mail: mvargas@ctima.uma.es

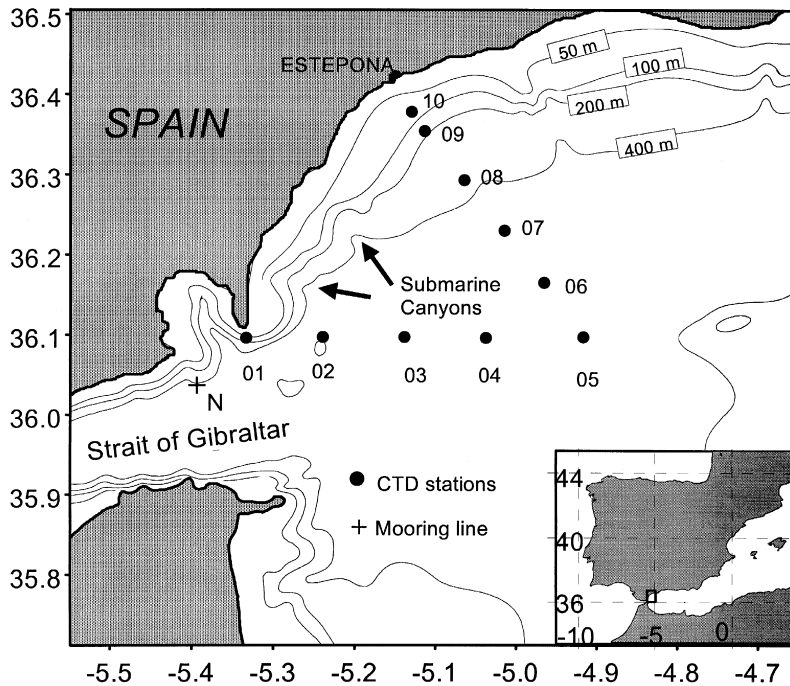


Fig. 1. Map of the Northwestern Alboran sea area showing the location of the oceanographic stations. Conductivity, temperature and depth (CTD) stations are indicated with dots and the mooring site with 'N'. Two important submarine canyons in the area have been marked by arrows.

ary of the upwelling area mentioned above. The strong gradient of properties between water north of the AJ and inside the Jet produces one of the most intense fronts of the Mediterranean Sea.

Upwelling can be forced by several mechanisms. The most evident is the one induced by winds, 'Ponientes' (westerlies) in this case. The water transported offshore sinks where it meets the less dense AJ water, so that the wind-driven upwelling should be more noticeable in areas near the coast.

Another important mechanism analysed in this paper is the upwelling related to the unsteadiness of the AJ-front position. It fluctuates in a north–south direction in connection with changes in the position and shape of the anticyclonic gyre (Cheney and Doblár, 1982; La Violette and Kerling, 1983; Parrilla and Kinder, 1987; Heburn and La Violette, 1990). For instance, Perkins et al. (1990) presented a situation in which the AJ was exiting the Strait of Gibraltar due East to bend toward the South within 60 km of the Strait. The Western Alboran Gyre was accord-

ingly small and the AJ was very displaced to the south, off our area of study. Such displacements would allow the water from below to upwell in order to fill the 'room' left behind. Of course, westward horizontal transport of surface waters north to the Jet should be considered as an alternative possibility. Note that this possibility would lead to the development of a cell of cyclonic circulation to the north of the southward drifting Jet, that will favour the presence of cold subsurface water near the surface due to the doming of isopycnals associated with anticlockwise circulation. Probably both types of motion are at work and complement each other. A similar mechanism has been proposed to explain the appearance of cold patches of water between the main path of the Gulf Stream and the shore (Lee et al., 1981). The development of meanders can lead to the formation of well defined cyclonic eddies with upwelled water at its centre. The possibility that the eddy is not fully achieved and the upwelled water remains separated from the shore by a filament of warm water to form

a ‘shingle’, in Chew’s (1981) words, cannot be disregarded. This situation recalls the backward circulation of surface waters commented above. Similar processes can take place in the northwestern portion of the Alboran Sea, with the north–south displacements of the AJ playing the role of the meanders. The magnitude of these displacements, tens of kilometres, suggests that large volume of water can be carried up to the surface.

There are other mechanisms that provide favourable conditions for upwelling. One of them is the interfacial friction of the AJ, with the underlying Mediterranean water, which is nearly motionless or flowing slowly in the opposite direction. Garret and Loder (1981) demonstrated that this friction, though small, can produce vertical motions in fronts that are geostrophically balanced to first order. Tintoré et al. (1991) used the ‘Q-vector’ formulation to show that upward motion takes place upstream of the anticyclonic gyre (upstream of a wave crest) and downward motion occurs downstream (upstream of a trough). Bower and Rossby (1989) observed this kind of circulation in the Gulf Stream meanders using neutrally buoyant floats.

Bottom topography provides favourable conditions for upwelling by two mechanisms as well. Blanton et al. (1981) showed that a flow over a shelf with curved and divergent isobaths is able to produce upwelling. A second mechanism is the presence of submarine canyons (Fig. 1), which are suitable conduits for exchange between shelf and deep basin (Hickey et al., 1983; Alvarez et al., 1996, among others). Garcia Lafuente et al., 1999b showed that a net flux of salt toward the shelf, driven by pressure gradients associated with internal tides, takes place through them. They put forward that other dissolved substances (nutrients for instance) would behave the same way.

The explanations above provide reasons for the almost-permanent presence of cold surface water in the area. Nevertheless, not all these mechanisms are equally important. For instance, vertical velocity estimated near our area of study, using the quasi-geostrophic Q vector formulation of the omega equation is of the order of 10^{-5} m s^{-1} (Viúdez and Tintoré, 1996). Vertical velocities of the order of 10^{-6} m s^{-1} were estimated in the continental shelf between Cape Hatteras and Cape Canaveral due to

isobath curving and divergence (Blanton et al., 1981). Fluxes driven by internal tides affect mainly the intermediate part of the water column. We think that two mechanisms will prevail: the wind driven upwelling (WU) and that due to north–south excursions of the AJ (DU).

The second mechanism is investigated in this paper that is organised as follows. Section 2 presents the data set and data processing. In Section 3 some results about the possibility of distinguishing the two types of upwelling from ‘in situ’ data is investigated. Section 4 presents some attempts to quantify the relative important of each one. Finally, Section 5 summarises our conclusions.

2. Data

2.1. CTD data

During the years 1996 and 1997, a series of oceanographic surveys were carried out in the Northwestern part of the Alboran Sea on board the R/V ‘Odón de Buen’ of the Instituto Español de Oceanografía (IEO). Conductivity, temperature and depth (CTD) profiles taken with a ‘SBE-25’ CTD probe equipped with a fluorescence sensor along the transects shown in Fig. 1 were repeated in the dates shown in Table 1. Salinity was evaluated using the practical salinity scale (PSS) and density calculated from the revised state equation by Millero and Poisson (1981). Data were filtered and subsampled to 1-m interval. Only the section perpendicular to the shore, formed by stations 05, 06, 07, 08, 09 and 10, is analysed here. It provides information on the cross-shore structure of the water column in which we are interested.

2.2. Time series

A mooring line deployed in position ‘N’ (see Fig. 1) provided information on the AJ properties at the eastern exit of the Strait of Gibraltar. The mooring line consisted of five conventional current meters (Aanderaa), equipped with conductivity and pressure cells, at nominal depths of: 40, 90, 170, 270 and 420 m, respectively. The servicing of the line was made during the surveys. The conditions under which the AJ entered the Alboran Sea, are thought to play an

Table 1

General information on the field experiment and other parameters of interest

Column 1 is the name assigned to each survey. Column 2 is the day when the survey was carried out. Column 3 is the distance from the shore to the front that identifies the northern edge of the AJ (see text). Column 4 is the salinity gradient at 20 m depth in the position assigned to the front, which gives an estimate of its intensity. Column 5 is the angle under which the AJ enters the Alboran Sea measured by the first currentmeter of the mooring line the day of the survey. It was evaluated from the low-passed series of velocity whose cartesian components are given in columns 6 and 7.

Survey	Date	Distance (km)	$\nabla S \times 10^{-5} \text{ m}^{-1}$	Angle	$U \text{ (cm s}^{-1}\text{)}$	$V \text{ (cm s}^{-1}\text{)}$
A1	22/04/96	29.0	7.1	6.8	30.0	3.5
A2	27/04/96	19.4	7.8	8.5	42.6	6.4
B1	07/07/96	26.9	5.6	13.1	50.0	11.7
B2	12/07/96	14.0 ^a	–	16.6	38.4	11.5
C1	07/12/96	26.7	8.2	17.1	37.4	11.5
C2	11/12/96	26.7	8.6	13.7	44.4	10.8
D1	19/02/97	> 40 ^b	–	5.3	34.7	3.2
D2	20/02/97	36.2	3.6	4.0	30.4	2.1
E1	03/05/97	35.0	5.1	4.5	25.6	2.0
E2	06/05/97	> 40 ^b	–	–6.51	35.0	–4.0
F1	20/07/97	37.4	6.1	^c	^c	^c
F2	22/07/97	> 40 ^b	–	^c	^c	^c

^aThe front position was determined by the maximum geostrophic vorticity in this survey.

^bThe front was beyond the outermost station of the transect ($D > 40$ km).

^cNo data from those days are available.

important role in the hydrological structure of our area. This is particularly true for the incoming angle, that is estimated from the slowly-varying (low-passed) velocity time series recorded by the uppermost currentmeter. Due to the periodic sinking of the line forced by the strong tidal currents in the Strait, the velocity time series recorded by a given instrument cannot be considered as taken at its nominal depth. This fact is of particular importance in a place like the Strait where the flow has a two-layered structure. Large vertical excursions can bring the uppermost currentmeter to the lower layer where the mean velocity flows opposite, what introduces a periodic bias in the measured current, obscuring its actual direction. Therefore, part of these observations must be rejected, so that the time series has not constant sampling interval any longer. The low passed time series are obtained by means of daily averages once the tidal contribution has been removed. Details of the process can be seen in the work of Garcia Lafuente et al. (1998).

2.3. Meteorological data

Local winds from Tarifa and Ceuta, in the Strait of Gibraltar, were obtained from the ‘Boletín Diario

del Instituto Nacional de Meteorología, Spain’. Ceuta records are influenced by local orography and they have been used exceptionally. An additional meteorological station was installed in Sotogrande port, next to Estepona (Fig. 1). Data from this station have been used when available.

3. Different upwelling events

The CTD data set has been analysed to investigate differences between WU and DU. The starting hypothesis is that each of them will uplift different types of water and will occur in different locations. WU would move up water that is on the continental shelf, colder and saltier than the water offshore due to mixing, while the water upwelled by DU is expected to be fresher and warmer. Accordingly, stations 10 and 09 on the shelf will be more sensitive to WU, and stations 08, 07, 06 and 05 to DU.

We anticipate an important difference between both mechanisms. A stationary situation of westerlies keeps WU at work, but a stationary location of the AJ does not produce DU. This is expected to be a transient feature that only happens when the AJ is drifting toward the south and does not depend on its

initial position. A hydrographic section helps to locate the AJ and the associated front, but it is not enough to identify DU. The drifting state of the AJ must be known. This is why currentmeter observations in the Strait are necessary.

3.1. Atlantic current through the Strait and the position of the front

We face the problem of locating the position of the AJ in order to follow their migrations to the south. The salinity minimum associated with the AJ

is probably the best indicator to trace its path through the Alboran Sea and in fact this criterion has been used (Viúdez and Tintoré, 1996). The limited offshore extension of the hydrological sections does not allow us to identify this salinity minimum unambiguously. Salinity gradient in the cross-shore direction is also a good indicator in order to locate the front (it is mainly a salinity front). The maximum of this gradient determines the position of the northern boundary of the AJ. Fig. 2 shows the offshore distance Y of this maximum evaluated at different depths. It is not sensitive to the selected depth and the accepted

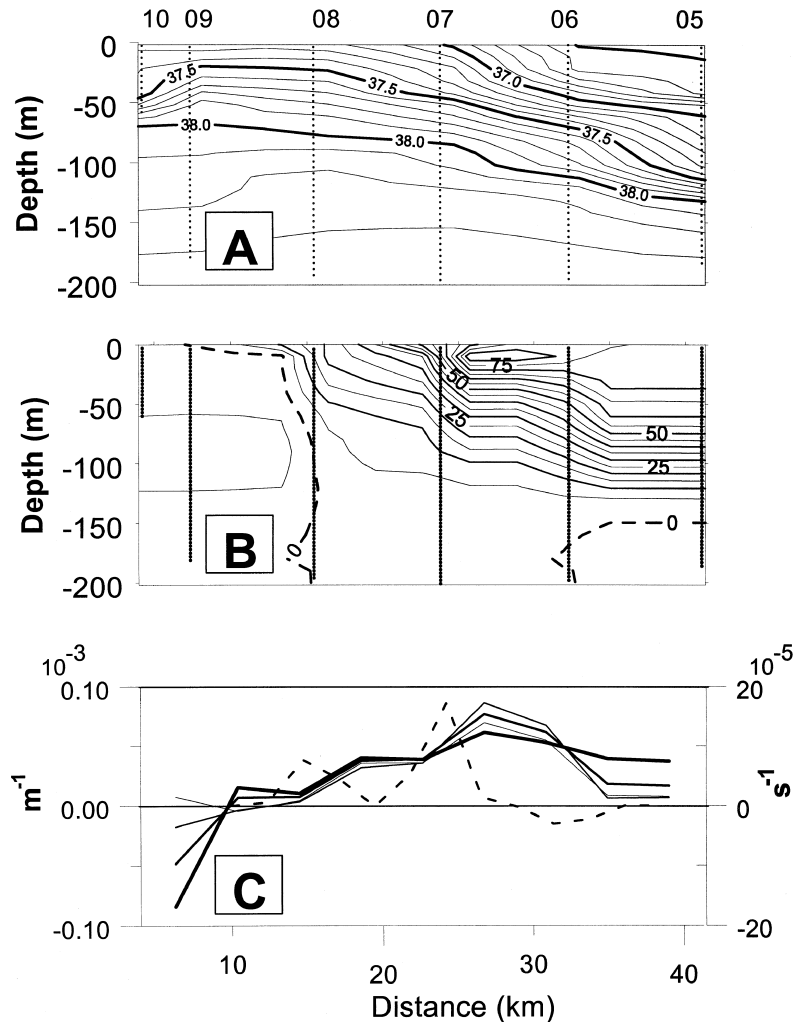


Fig. 2. (A) Contours salinity and (B) contours of geostrophic velocity obtained during C2 survey. (C) Salinity gradient at different depths (solid lines), and relative geostrophic vorticity at 20 m depth during the same survey (dashed line).

distance was that obtained at 20 m depth. Table 1 shows this distance for the different surveys. Sometimes the maximum gradient of salinity is not well defined and the calculation of the distance by this method is not suitable. Survey B2 is an example. The maximum gradient of along geostrophic velocity (maximum relative geostrophic vorticity) is an alternate criterion. This calculation involves one numerical step more than the computation of $(\partial S / \partial Y)$ and, therefore, it is more sensitive to numerical errors. For this reason salinity criterion will be used whenever possible. Note in Fig. 2 that both methods provide similar, though not equal results.

Fig. 3 is a scatter diagram of distance Y against the incoming angle α of the AJ measured in site 'N' (positive counterclockwise). A linear fit of the form $Y = A + B\alpha$ gives 36.6 ± 4.9 km and -0.94 ± 0.42 km degrees⁻¹ (54 ± 24 km radians⁻¹) for parameters A and B , respectively, with a regression coefficient of -0.67 . This coefficient improves to -0.78 if we exclude the data corresponding to survey C1 (point inside the rectangle in Fig. 3) which has abnormally high angle. The new values for A and B are 38.8 ± 4.8 km and -1.26 ± 0.45 km degrees⁻¹ (72 ± 25 km radians⁻¹).

The linear model above can be understood as the classical relation between arc Y and angle α , in which case B should play the role of the circle radius. It should match the distance from point 'N'

to the hydrographic section. Fig. 1 indicates that this of 50 km, while B is around 72 km. Despite the weak agreement, the actual distance is still inside the error interval of B and we accept the linear model as representative (the value of B in the first fitting is closer to 50 km, however, we still consider its last value because the regression coefficient gives more confidence to the fitting). Therefore, the low passed time series of velocity in site 'N' indicates the drifting situation of the front and the AJ, in particular during the days before a given survey was carried out. Note that even if the actual relationship between Y and α were more complicated (and probably it is) the previous statement is still meaningful: if α decreases, the front and AJ migrate to the south and vice versa.

3.2. AJ position and upwelling

Surveys A1 and C1 have been selected to illustrate upwelling events. Panels A to C of Fig. 4 show sections of temperature along with fluorescence, salinity and geostrophic velocity, respectively, during A1. High fluorescence values indicate high chlorophyll and phytoplankton biomass concentration. As known, this biomass can only achieve high concentrations when nutrients are supplied to the photic zone, mainly by upwelling.

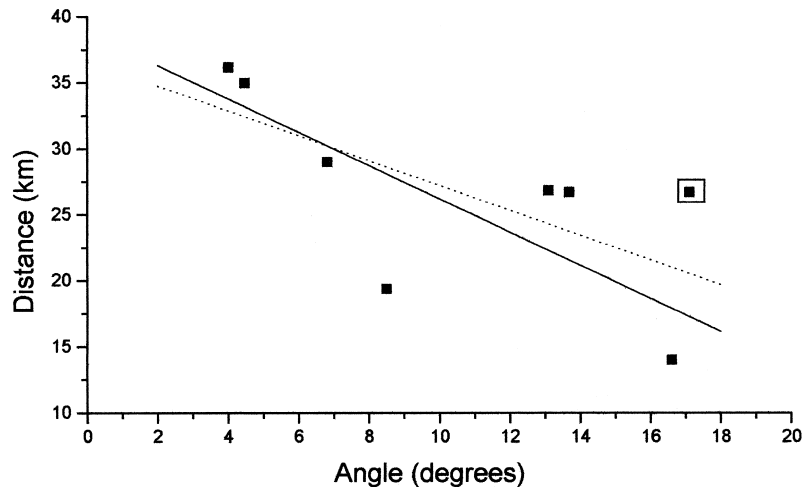


Fig. 3. Dispersion diagram between the distance of the front to the coast and the incoming angle. Dashed line is the fitting with all data points. Solid line is the fitting without the data inside the rectangle.

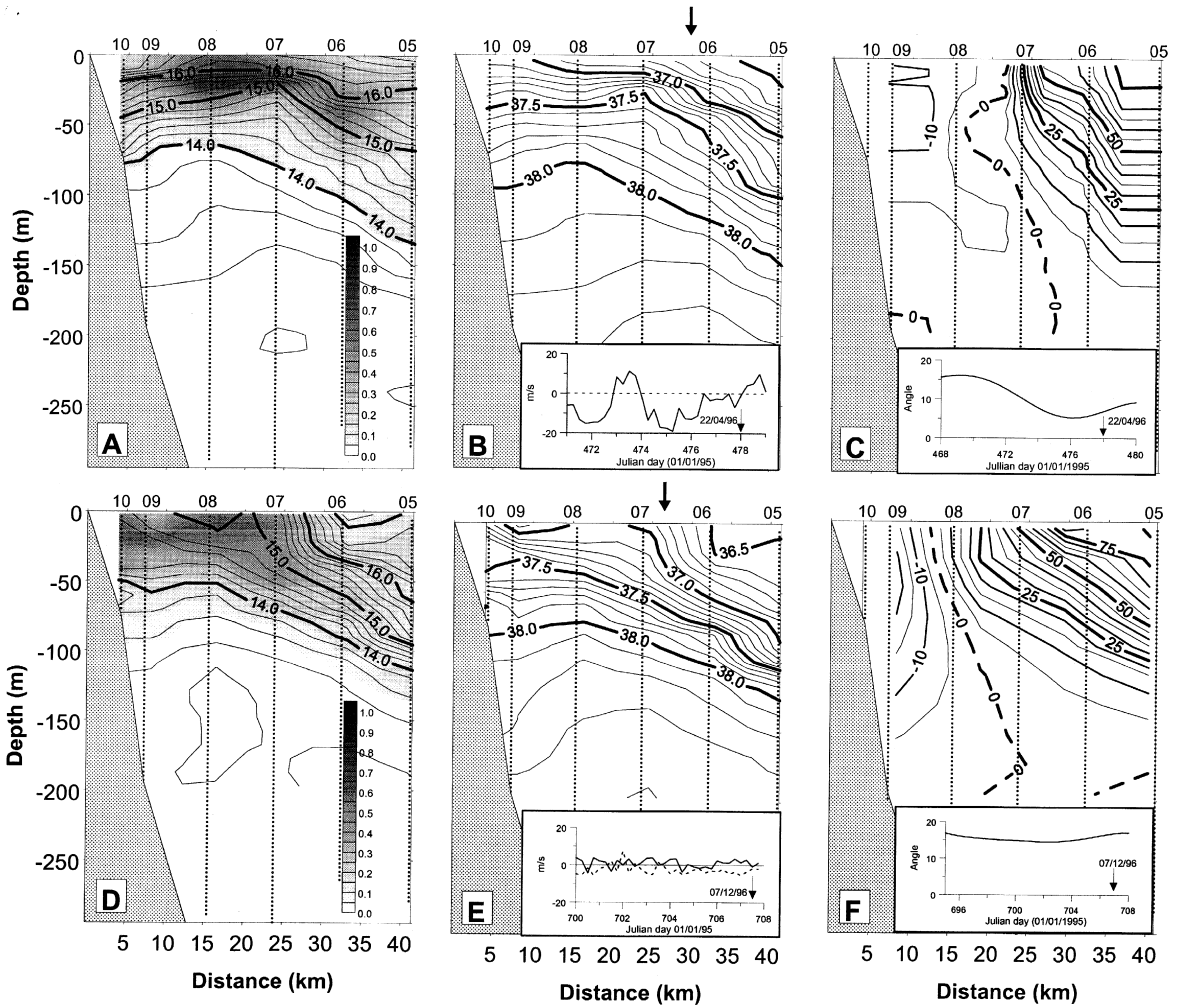


Fig. 4. (A) Temperature (contours) and fluorescence (filled areas), (B) salinity and (C) geostrophic velocity during survey A1 respectively. Insert on panel B is the zonal component of the wind measured in Tarifa (positive values indicate westerlies). Insert on panel C shows the incoming angle in the mooring site. (D, E and F) Same as (A, B and C) for survey C1. Insert on panel (E) gives the zonal (solid line) and northward (dotted line) components of wind measured in Sotogrande.

Panel A in Fig. 4 shows that isotherms dome around stations 07 and 08. Geostrophic velocity suggests a cyclonic circulation centred at these stations. Fluorescence is high here and it diminishes shoreward and seaward. All this gives support to the existence of upwelling near the centre of the section.

The reason for this high fluorescence value has to be searched in some events previous to the survey, because fitoplankton response lags favourable conditions for upwelling some days (Mann and Lazier, 1991, p. 180). Insert in Fig. 4C presents the time

evolution of the incoming angle α . It started decreasing 1 week before the survey and went on diminishing until the day before the survey. That implies a southward displacement of the front during this period. Insert in panel 4B shows that wind was blowing from the east during the previous week, except for 1 day just 4 days before the survey. So that, this upwelling event is more likely related to DU, rather than to WU.

During C1 survey, the front was quite well defined by temperature and salinity. It was in a similar

position as in A1 survey. Geostrophic velocity indicates cyclonic circulation again. Fluorescence was high all over the section but particularly near the shore. Insert in Fig. 4E shows that westerlies or northwesterlies were blowing before the survey, and went on blowing during it. The upward bend of isotherms and isohalines near the shore and the above-mentioned high value of fluorescence point at a clear WU event. Salinity and temperature vertical sections also suggest upwelling in the middle of the section. Fluorescence confirms the existence of upwelling too. Apparently the upwelling in the middle of the section cannot be related to DU, since the front was slowly approaching to shore during the survey as can be seen in the insert of Fig. 4F. However it was drifting to the south during a long period before the survey (days 695–703 approximately). The possibility remains that the traces of upwelling could be the effects of that southward migration. We need additional information to decide whether or not it has connections with a DU event.

To further investigate this subject, we have developed a method based on fluorescence measurements

to classify upwelling events. Fig. 4A and D shows that, for a given depth, high fluorescence values correspond to low temperature values. This is better seen in Fig. 5. Accordingly, we select samples in which fluorescence is above a threshold value. These samples are assumed to correspond with upwelled water and their T–S characteristics are then analysed with the help of a T–S diagram.

Fig. 6 shows the results of this method for different surveys using a threshold value of 80% of the maximum of fluorescence found during the survey to discriminate samples. Two clouds are detected during C1. The first one is shifted toward high salinity and low temperature values, the samples being from stations 09 and 10. All this confirms the continental shelf nature of the upwelled water that will be related to WU events. The second cloud is centred at lower values of salinity and higher values of temperature. The samples come from stations 07 and 08. The upwelled water seems to have a different source now. Similar analysis for A1 survey, when we found a clear DU event, gives a unique cloud located around the same salinity value and with the same

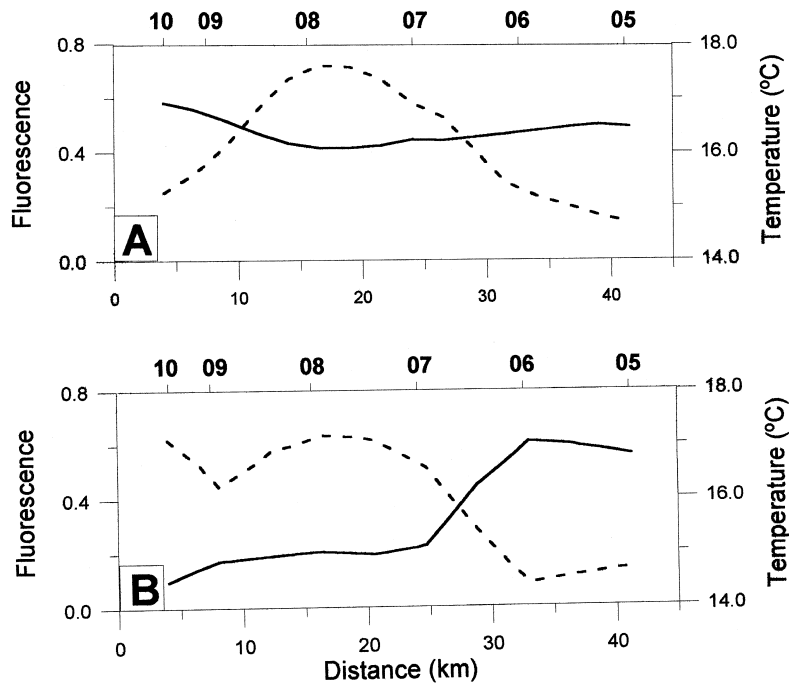


Fig. 5. (A) Temperature (solid line, right scale) and fluorescence (dashed line, left scale) at 10 m depth during survey A1. (B) Same as in (A) during survey C1.

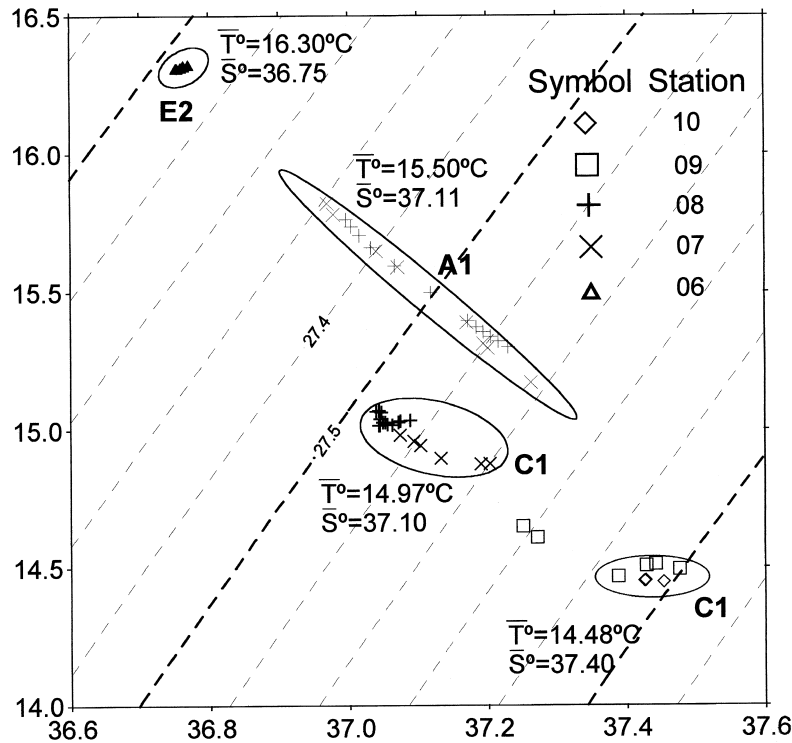


Fig. 6. T–S diagram including only points with fluorescence higher than a certain value (see text), during different surveys.

stations as in the second cloud for C1 involved. Temperature is higher, what can be explained by seasonal variability, because A1 was made on April and C1 on December. In any case, it appears that both clouds (second of C1 and A1) have similar origin: relative fresh and warm water.

Another illustrative example is supplied by surveys E1 and E2 carried out four days apart. Fig. 7B shows a front between stations 06 and 07. Four days later, the front was not detected (Fig. 7D). The insert in Fig. 7D indicates that the AJ was drifting to the south quickly. Accordingly, surface temperature decreased from E1 to E2. The infrared image of Fig. 7E, taken between both surveys, depicts an AJ coming into the Alboran Sea following a much more southward path than usual. The mentioned method produces the narrow cloud of points in the upper-left corner of Fig. 6 for E2 and gives support to a strong DU event.

We applied the Student's *t*-test to investigate whether the mean values that appear beside the clouds on Fig. 6 are statistically different. If only

salinity is considered to define these clouds, then A1 and the second of C1 clouds are not statically different (obviously), while all others are different at a 95% of significance. On the contrary, if T–S characteristics are used to define then, all clouds are statistically different at 95% of significance. Allowing for seasonal variability in temperature, the analysis above points at the same source for the upwelled waters in stations 07 and 08 during A1 and C1, suggesting DU upwelling for both events.

The results above indicate that it is possible to distinguish between both types of upwelling. Sometimes, however, the difference is not so clear, but a gradual transition takes place instead. Survey D1 is an example. Westerlies were blowing since 1 week before the survey started (see insert in Fig. 8A) and the AJ was migrating to the south (insert in Fig. 8B). It is not surprising to find a generalised upwelling in the whole area under these favourable conditions. Fig. 8A shows that surface temperature is low and homogeneous. Fluorescence is slightly higher in coastal stations what can be interpreted in terms of

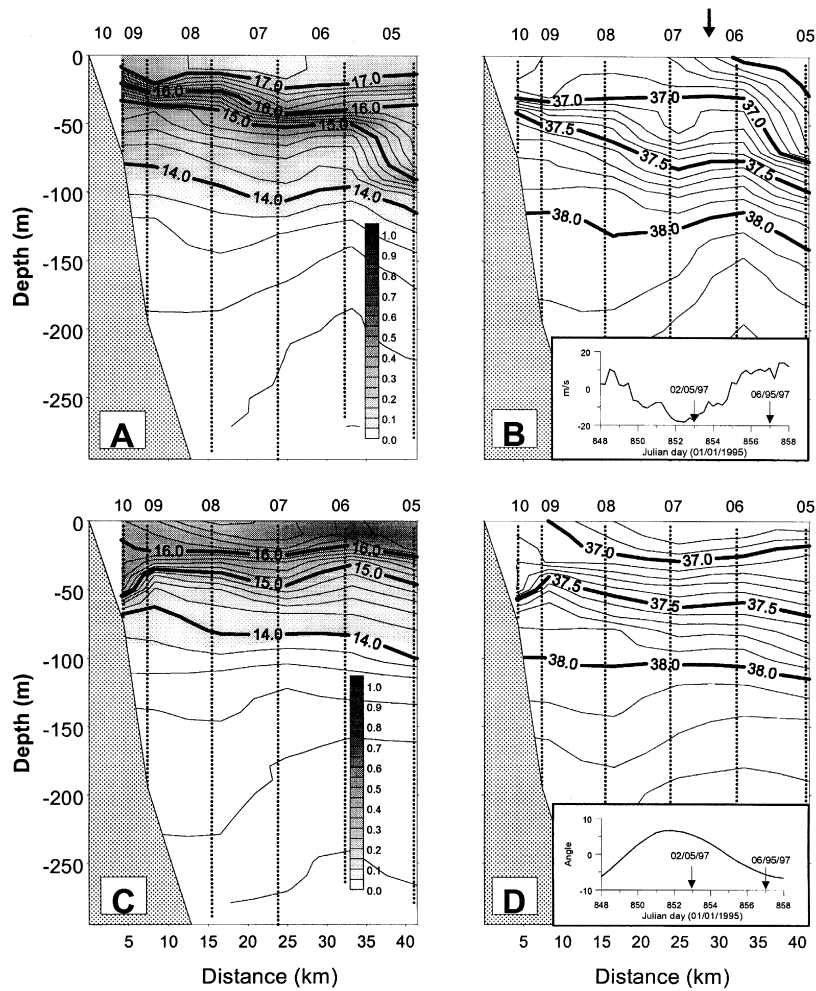


Fig. 7. (A) Temperature and fluorescence and (B) salinity during survey E1 (see also caption in Fig. 4). (C and D) Same as (A and B) for survey E2. Insert of panel (B) is zonal wind measured in Tarifa and insert in (D), is the incoming angle. (E) Infrared image of the area taken by NOAA-14 on 04/05/97. Note the 'anomalous' path of the AJ at the exit of the Strait of Gibraltar.

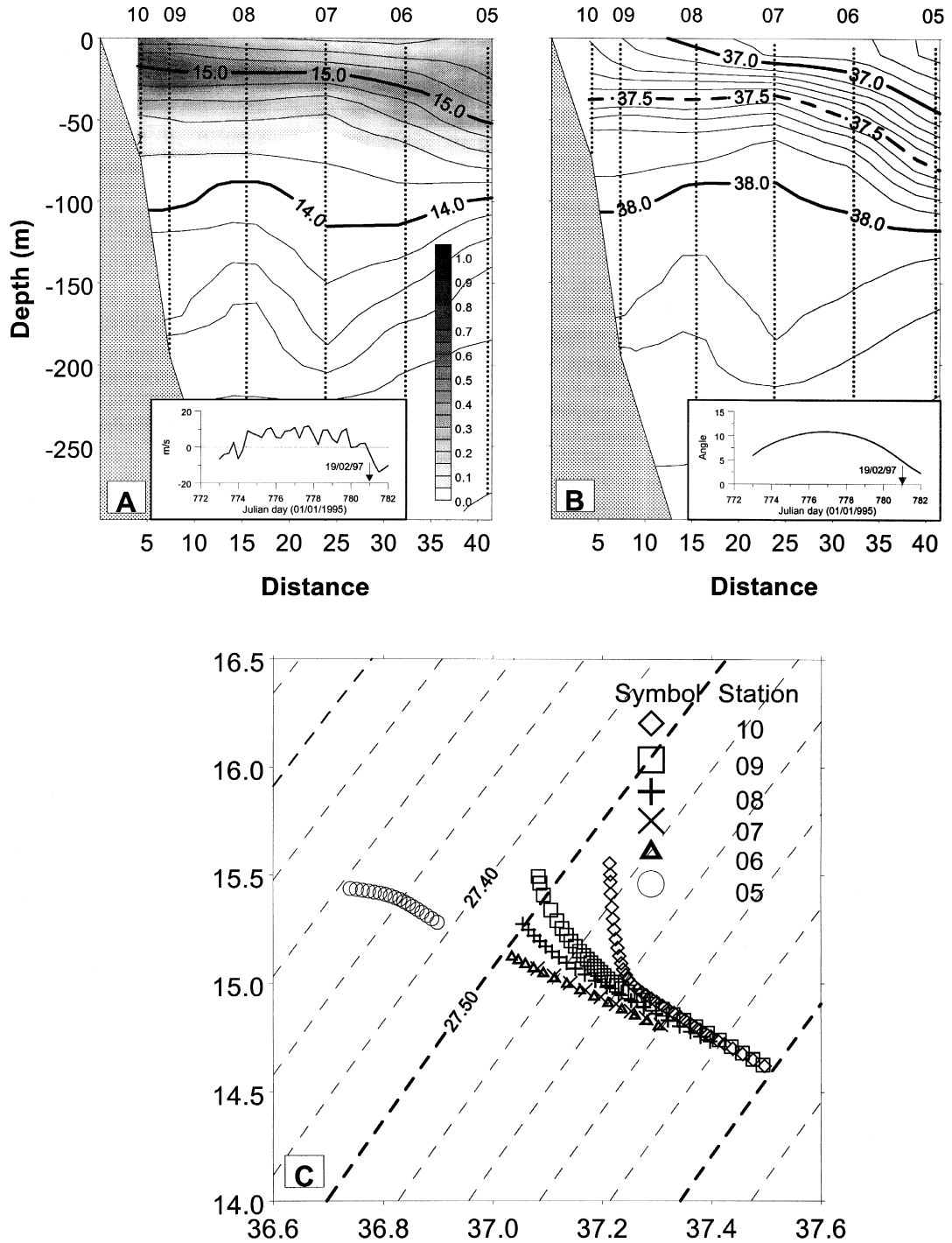


Fig. 8. (A) Temperature and fluorescence and (B) salinity profiles during D1 survey, respectively. (C) T–S diagram of data points with fluorescence greater than 0.4. Insert in (A) and (B) are zonal wind measured in Tarifa and angle of the AJ, respectively.

the persistence of westerlies against the recent drifting of the AJ to the south. The T–S characteristics of samples with fluorescence higher than 0.4 are shown in Fig. 8C. A gradual transition from continental shelf water in station 10 to relative fresh and warm atlantic water in station 05, farther offshore, is evident.

4. Discussion

In Section 3, the possibility of distinguishing both types of upwelling from CTD data has been investigated. Next, we make some estimations to assess their relative importance. The vertical velocity of a wind-driven upwelling in a simple coastal upwelling model is given by (see Fig. 9A)

$$w_{\text{WU}} = \frac{\tau}{\rho f L} \quad (1)$$

where ρ is the water density, f is the Coriolis parameter, L is a cross-shore length scale of up-

welling and τ is the wind-stress, which is usually estimated as

$$\tau = \rho_a C_d V^2 \quad (2)$$

where ρ_a is the density of the air, C_d is the drag coefficient and V the wind speed.

A choice of L could be the distance from the shore to the point where $S = 37.0$ intersects the free surface. Using information from those surveys when WU was documented to be at work, the condition above is met in the surroundings of station 08, so that L would be of the order of 18 km. With $\rho_a = 1.3 \text{ kg}^{-3}$, $\rho = 1028 \text{ kg}^{-3}$, $f = 8.5 \times 10^{-5} \text{ s}^{-1}$, $C_d = 2.6 \times 10^{-3}$ (Mann and Lazier, 1991), a wind of 10 m s^{-1} will produce a vertical velocity of $2.1 \times 10^{-4} \text{ m s}^{-1}$ or 18 m day^{-1} .

To estimate the averaged amount of upwelled water during a year, we have to determine the frequency of westerlies. Fig. 10 is a scatter diagram of daily wind direction observed in Tarifa for a period of 3 years. The percentage of westerlies is 50.5%, in agreement with May's (1982) map of wind stress over the Mediterranean. To have an estimate of V^2 for Eq. (2) we have calculated the mean of V_{iw}^2 where subindex 'iw' refers to the subseries of westerlies within the wind time series. We obtain $\langle V_{\text{w}}^2 \rangle = 51 \text{ m}^2 \text{ s}^{-2}$ and a mean vertical velocity of 9.5 m day^{-1} , which in turn implies an annual vertical flux of $31 \times 10^6 \text{ m}^2$ per length unit parallel to the coast.

Let us consider now the situation sketched in Fig. 9B, in order to make estimations for DU. Shadowed area is the cross section of the AJ whose typical thickness is H . The AJ drifts a distance R , perpendicularly to the shore from position 1 to 1'. If the 'room' left by the AJ is filled by water from below, a volume RH per unit length parallel to the shore must upwell during the time T it takes the AJ to migrate. Under this simple hypothesis, the average vertical velocity in the area affected by the drift would be $w_{\text{DU}} = H/T$, which is an overestimation since some surface recirculation is expected to occur.

The thickness H can be estimated as the depth of $S = 37.5$ isohaline in vertical sections of salinity. If so, $H \sim 80 \text{ m}$ is a representative value. A spectral analysis of the time series of the incoming angle α , shows a dominant peak around 16 days (Fig. 11), what allows us to assign 8 days to T (southward drifting). Then we obtain $w_{\text{DU}} \sim 10 \text{ m day}^{-1}$ (~ 1.1

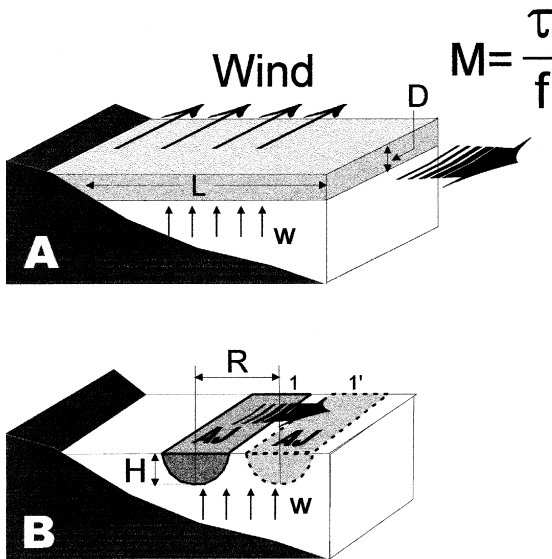


Fig. 9. (A) Sketch of wind-induced upwelling. A wind-stress τ produces a transport of mass per unit length parallel to the shore of $M = \tau/f$. Continuity considerations lead to the vertical velocity given by Eq. (1), which does not depend on the thickness of the Ekman layer D . (B) Sketch of an offshore drifting of length R of the AJ.

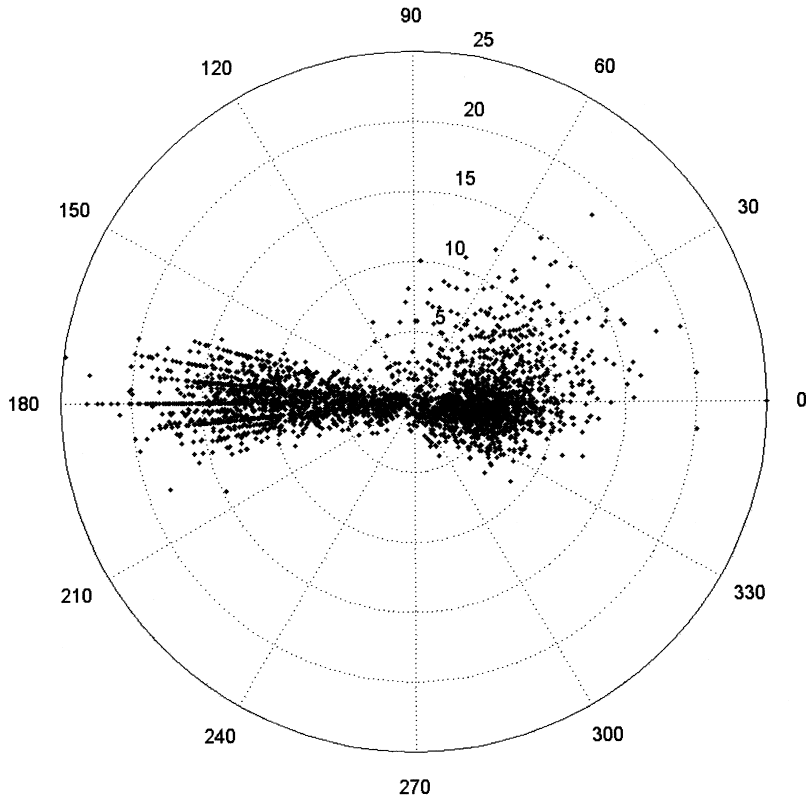


Fig. 10. Scatter diagram of wind velocities in Tarifa for the years 1995 to 1997.

$\times 10^{-4} \text{ m s}^{-1}$) of the same order as w_{WU} . A typical value for R , which is necessary to estimate the volume of upwelled water, is obtained from the linear relation of the previous section taking an angle equal to twice the standard deviation of the series of α . We obtain 11.4 degrees and $R = 14.3 \text{ km}$ using the second estimate of B .

In order to calculate the annual volume of water lifted by DU we need to know how many southward drifting events happen on average during a year. Taking centred differences in the time series of α , we obtain that 44% of the times, the angle decreases (what means southward drifts), 45% it increases and 11% it appears to be steady. Therefore, southward displacements happen during 160 days each year on average, and a vertical flux of $23 \times 10^6 \text{ m}^2$ per length unit parallel to the coast is finally obtained.

According to these results, both types of upwelling are of the same order. We are aware of the roughness of our computations, particularly in the

case of DU. Anyway, we believe that WU is able to upwell larger amount of water than DU, a conclusion that is supported by our estimations if we take into

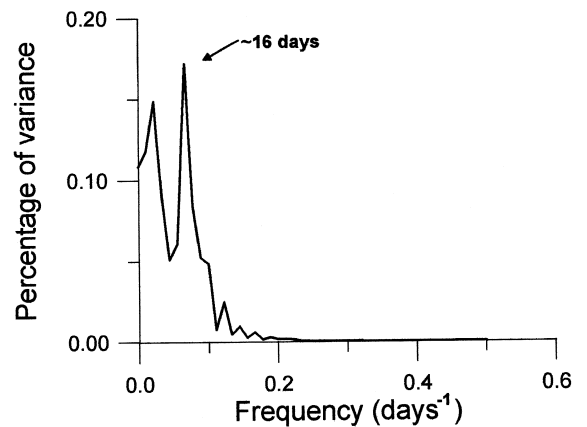


Fig. 11. Spectral density of the angle, under which the AJ enters the Alboran Sea, measured in site N.

account the upper-limit computations carried out to assign a value to w_{DU} .

Even when the quantity of water was of the same order, its quality is different from a biological point of view. Nutrient concentration in this area exhibits a clear trend to decrease from coast to offshore. Averaged value of $[\text{NO}_3]^-$ concentration in the area where WU is expected to prevail is $5 \mu\text{mol/l}$ and it decreases to $3 \mu\text{mol/l}$ in the area where DU is more important (A. Reul, personal communication). That means that 9.6 and 4.3 tons m^{-1} of NO_3 are pumped to the surface by WU and DU, respectively. Therefore, WU is more important to fertilize surface waters in the area. However the contribution of DU cannot be neglected since it can account for up to 50% of the former.

5. Conclusions

The goal of this paper was to investigate the relative importance of two different types of upwelling that are thought to be important in the fertilization of surface waters in the northwestern area of the Alboran Sea. Additionally to the well-known mechanism of wind-driven upwelling, we have shown that southward drifts of the AJ also have a significant contribution to the upwelled water. We found reasonable good correlation between the angle under which the Jet enters the Alboran Sea and the distance from coastline to the north edge of the AJ. Thus, the displacements of the Jet can be tracked by this angle, a result that helps estimating the effectiveness of DU.

A method to differentiate WU and DU has been developed based on the different T–S characteristics of the water upwelled either mechanisms. The events of upwelling have been identified using a criterion based on the registered fluorescence. When westerlies blow, high values of fluorescence are found near the shore, and the water is relatively salty and cold. When southward migrations of the AJ are detected, high values of fluorescence are found offshore, and the water associated in this case is warmer and fresher.

Some quantitative estimates of the importance of these two types of upwelling have been carried out. Vertical velocities associated to both of them are

comparable and they are one order of magnitude higher than those associated to any other mechanisms commented in the introduction. This indicates that WU and DU play a predominant role in the upwelling dynamic of the region. WU seems to be more important than DU because its area of influence appears to be somewhat larger and, particularly, because the water it lifts has higher nutrient concentration. However DU events can pump up to the surface as much as 50% of the nutrients upwelled by WU. Moreover, it occurs in areas where WU cannot affect. Sporadic situations of sudden and large migrations of the Jet to the south would be the most important mechanism for upwelling, especially under weather calm conditions.

Acknowledgements

The oceanographic surveys were carried out in the R/V *Odon de Buen* from the Instituto Español de Oceanografía (IEO). We thank its crew for their altruistic help. This study has been funded by CI-CYT (MAR95-1950-C02-01) and also by MATER-MTPII and CANIGO projects. T. Sarhan was supported by a FPI fellowship from Ministerio Español de Educación. J.M. Vargas and F. Plaza acknowledge fellowships from MAS3-CT96-0051 and MAS3-CT96-0060 respectively. The authors wish to thank A. Reul for providing nutrients data.

References

- Alvarez, A., Tintore, J., Sabates, A., 1996. Flow modifications and shelf-slope exchange induced by a submarine canyon off the Northeast Spanish Coast. *J. Geophys. Res.* 101, 12043–12055.
- Blanton, J.O., Atkinson, L.P., Pietrafesa, L.J., Lee, T.N., 1981. The intrusion of Gulf Stream water across the continental shelf due to topographically-induced upwelling. *Deep Sea Res.* 28A (4), 393–405.
- Bower, A.S., Rossby, T., 1989. Evidence of Cross-Frontal Exchange process in the Gulf Stream based on isopycnal RAFOS float data. *J. Phys. Oceanogr.* 19, 1177–1190.
- Cano, N., 1977. Resultados de la campaña 'Alborán 73'. *Bol. Inst. Esp. Oceanogr.* Tomo I, 103–176, Enero.
- Cheney, R.E., Doblar, R.A., 1982. Structure and variability of the Alboran Sea Frontal System. *J. Geophys. Res.* 87 (C1), 585–594.

- Chew, F., 1981. Shingles, spin-off eddies and an hypothesis. *Deep Sea Res.* 28A (4), 379–391.
- Copin-Montegut, G., Coste, B., Gascard, J.C., Gostan, J., Le Corre, P., Minas, H.J., Packard, T.T., Poisson, A., 1982. Nutrient regeneration and circulation patterns in the Strait of Gibraltar and the Western Mediterranean Sea. *Abstr. ESO* 63 (3), 109.
- García Lafuente, J., Vargas, J.M., Cano, N., Sarhan, T., Plaza, F., Vargas, M., 1998. Observaciones de corriente en la estación 'N' en el Estrecho de Gibraltar desde Octubre de 1995 a Mayo de 1996. *Inf. Tec. Inst. Esp. Oceanogr.* 169, 46 pp.
- García Lafuente, J., Vargas, J.M., Plaza, F., 1999a. The tide at the eastern section of the Strait of Gibraltar. *JGR*, Submitted.
- García Lafuente, J., Sarhan, T., Vargas, M., Vargas, J.M., Plaza, F., 1999b. Tidal motions and tidally-induced fluxes through La Línea Submarine Canyon, Western Alboran Sea. *J. Geophys. Res.* 102 (C2), 3109–3119.
- Garret, C.J.R., Loder, J.W., 1981. Dynamical aspects of shallow-sea fronts. *Philos. Trans. R. Soc. London A* 302, 562–581.
- Heburn, G.W., La Violette, P.E., 1990. Variations in the structure of the Anticyclonic Gyres found in the Alboran Sea. *J. Geophys. Res.* 95 (C2), 1599–1613.
- Hickey, B., Baker, E., Kachel, N., 1983. Suspended particle movement in and around Quinault submarine canyon. *Mar. Geol.* 71, 35–83.
- Lanoix, F., 1974. *Projet Alboran. Etude hydrologique et dynamique de la mera d'Alboran.* Tech. Rep., 66, N. Atl. Traty Org. Brussels.
- La Violette, P.E., 1984. The advection of cyclic submesoscale thermal features in the Alboran Sea Gyre. *J. Phys. Oceanogr.* 14 (3), 550–565.
- La Violette, P.E. and Kerling, J.L., 1983. An analysis of aircraft data collected in the Alboran Sea during 'Donde Va?', October 1982. *NORDA. Tech. Note* 222, 126 pp.
- Lee, T.N., Atkinson, L.P., Legeckis, R., 1981. Observations of a Gulf Stream frontal eddy on the Georgia continental shelf, April 1977. *Deep-Sea. Res.* 28A (4), 347–378.
- Mann, K.H., Lazier, J.R.N., 1991. *Dynamics of Marine Ecosystems.* Blackwell.
- May, P.W., 1982. Climatological Flux estimates in the Mediterranean Sea: Part I. Winds and Wind Stress. *Naval Ocean Research and Development Activity Technical Report*, 54, 59 pp. NSTL Station, Mississippi 39529.
- Millero, F.J., Poisson, A., 1981. International one-atmosphere equation of state of sea water. *Deep-Sea Res.* 28, 625–629.
- Parrilla, G., Kinder, T., 1987. *Oceanografía física del mar de Alborán.* *Bol. Inst. Esp. Oceanogr.* 4 (1), 133–165.
- Perkins, H., Kinder, T., La Violette, P., 1990. The Atlantic inflow in the Western Alboran Sea. *J. Phys. Res.* 20, 242–263.
- Rodríguez, V., Bautista, B., Blanco, J.M., Figueroa, F.L., Cano, N., Ruiz, J., 1994. Hydrological structure, optical characteristics and size distribution of pigments and particles at a frontal station in the Alboran Sea. In: Rodríguez, J., Li, W.K.W. (Eds.), *The Size Structure and Metabolism of the Pelagic Ecosystem.* *Sci. Mar.* 58, pp. 31–41.
- Rubín, J., Rodríguez, V., Blanco, J., Jiménez-Gómez, F., Rodríguez, J., Lafuente, J.G., Echevarria, F., Guerrero, F., Escanez, J., Hernandez, A., Chabani, M., 1995. Relaciones del ictioplancton con la hidrología, biomasa fitoplanctónica, oxígeno disuelto y nutrientes en el Mar de Alborán y Estrecho de Gibraltar (Julio 1993). *Publ. Esp. Inst. Esp. Oceanogr.* 24, 75–84.
- Rubín, J., Cano, N., Arrate, P., Lafuente, J.G., Escanez, J., Vargas, M., Alonso, J., Hernandez, S., 1997. Ictioplancton, el mesozooplancton y la hidrología en el Golfo de Cádiz, Estrecho de Gibraltar y sector Noroeste del Mar de Alborán de Julio de 1994. *Inf. Téc. Inst. Esp. Oceanogr.* 167, 44 pp.
- Tintoré, J., Gomis, D., Alonso, S., 1991. Mesoscale dynamics and vertical motion in the Alboran sea. *J. Phys. Res.* 21, 811–823.
- Viúdez, A., Tintoré, J., 1996. Circulation in the Alboran Sea as determined by quasi-synoptic hydrographic observations: Part I: Three-dimensional structure of the two anticyclonic gyres. *J. Geophys. Res.* 26 (5), 684–705.